

# PREDICTION OF THE ACOUSTIC INFLUENCE OF AN INTAKE ON FAN FLUTTER: A COMPARISON OF NUMERICAL METHODS

*T. Bontemps*<sup>a, b</sup>, *S. Aubert*<sup>a</sup>, *N. de Cacqueray*<sup>b</sup>

a: Université de Lyon, ECL, LMFA, UMR CNRS 5509, 69131 Ecully, France

b: Safran Aircraft Engines, 77550 Moissy-Cramayel, France

thomas.bontemps@ec-lyon.fr

stephane.aubert@ec-lyon.fr

nicolas.de-cacqueray@safrangroup.com

## ABSTRACT

In certain operating conditions, acoustic propagation and reflection in air intake may have an influence on fan flutter. This paper presents an analytical low fidelity model to evaluate unsteady pressure wave reflected by the inlet. To understand possibilities and limitations of this model, it is compared to acoustic finite element simulations. Although an excellent agreement was found between the model and numerical simulations for a cylindrical intake, quite important gaps are observed for an intake with large lips. The pressure amplitude ratio is globally overestimated and phase lag is obtained with a low precision. The main problematic element seems to be the curved shape of intake lips. Nevertheless, predictions are good enough to locate zones over the compressor map that correspond to a potentially destabilizing phase lag. Possible improvements are the usage of a meridional field as an input to the model and a more accurate modelling of cut-off to cut-on transition.

## KEYWORDS

Fan flutter, fan/intake interaction, acoustic reflection

## NOMENCLATURE

$A_m^\pm$	Amplitude of the outgoing (–) or incoming (+) mode ( $m, 0$ )	$p_m^\pm$	Pressure outgoing (–) or incoming (+) mode ( $m, 0$ )
$a$	Sound speed [m/s]	$r$	Radius [m]
$f$	Flutter frequency [Hertz]	$r_0$	Reference radius [m]
$f_c$	Cut-on frequency [Hertz]	$\mathcal{R}$	Reflection rate
$i$	Imaginary unit, $i^2 = -1$	$t$	Time [s]
$k$	Wave number [ $m^{-1}$ ]	$x, \xi$	Axial position [m]
$K_m$	Radial wave number [ $m^{-1}$ ]	$\mu$	Radial order
$k_x$	Axial wave number [ $m^{-1}$ ]	$\omega$	Flutter angular frequency [rad/s]
$m$	Nodal diameter / Azimutal order	$\phi$	Phase [deg]
$\dot{m}$	Massflow [kg/s]	$\Delta\phi$	Phase lag [deg]
$\dot{m}_0$	Reference massflow [kg/s]	$\psi_m$	Radial distribution of the mode ( $m, 0$ )
$M_x$	Axial Mach number	$\theta$	Azimutal angle
$p$	Acoustic pressure [Pa]	$\tau$	Pressure amplitude ratio

## INTRODUCTION

Flutter is an aeroelastic instability that may occur on various operating conditions and can lead to failure by fatigue. Fan design requires to predict correctly flutter conditions, but the underlying mechanisms of this phenomenon are still misunderstood. Many authors studied the influence of local aerodynamic structures around the blade, such as shock wave / boundary layer interaction, like Aotsuka and Murooka (2014). However, impact of acoustic coupling between fan flutter and its surroundings is often not considered. Whitehead (1973) showed early the possibility of an ‘acoustic resonance flutter’ occurring around duct cut-on frequency. This idea is developed since the 2000’s, for instance by Vahdati et al. (2011), Vahdati et al. (2015) and Vahdati and Cumpsty (2016). They distinguish two types of stall flutter, occurring near the stall line. The first one is a classical aerodynamic stall flutter, due to the local aerodynamic field around the blade. The second type is what they call acoustic driven flutter. It is due to propagation and reflection of an acoustic wave emitted by fan vibration that interacts with flutter. Indeed, under certain conditions, acoustic waves generated by fan vibration can propagate upstream in the engine intake, and be partly reflected on the intake opening. Eventually, waves propagate downstream back to the fan and interact with fan vibration with a phase lag. Figure 1 illustrates this mechanism. If the wave comes back on the fan with a particular phase, it can destabilize it enough to trigger flutter. In the quite narrow zone where this phenomenon occurs near cut-on frequency of the intake, flutter margin is reduced in what they call flutter bite.

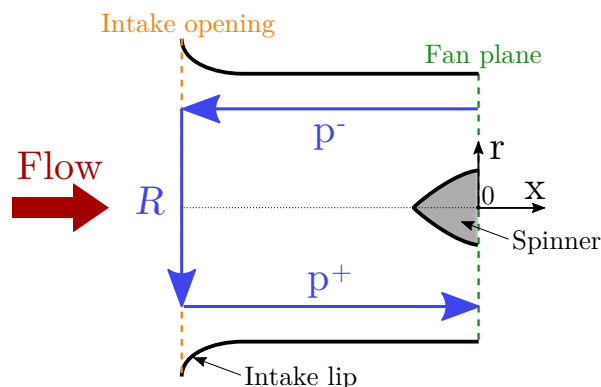


Figure 1: **Acoustic propagation and reflection in the intake.**  $p^-$ : outgoing wave,  $R$ : reflection,  $p^+$ : incoming wave

Thus, it might be important to take this aspect into account for fan and engine design. In particular, parameters like intake length, shape and acoustic treatments require a particular attention. To integrate this phenomenon, new methodologies have to be developed. Firstly, Navier-Stokes 3D computations can be carried out, to simulate both the intake and the fan. However, it requires to choose very carefully the numerical setup, and its cost could be prohibitive for industrial design. Secondly, one can use a numerical acoustic solver to compute the acoustic field in the intake. Vallon et al. (2018) used vibroacoustic simulations to investigate the feed-back of acoustic on flutter for an helicopter impeller. The acoustic damping is computed considering the vibrating response of the impeller to imposed acoustic modes. Lastly, Zhao et al. (2017) built an analytical model to predict influence of intake on fan flutter. With a simple intake geometry and perfectly rigid walls, it seems to be well-suited to assess if intake has a stabilizing or destabilizing effect on fan flutter.

To locate operating points where fan flutter may occur, one may be interested in knowing the acoustic behavior of the intake in response to a given mechanical mode with a given nodal diameter. To do so for various massflows and rotating speeds, which can be related to the mechanical mode frequency, this paper aims to compare an analytical model to acoustic numerical results. The main objective is to understand limitations of the model and how to improve it, in order to obtain an effective low-fidelity solution for preliminary design. The first two parts introduce the analytical model and the acoustic solver Actran. Then both are compared for a given massflow and a varying frequency, firstly to validate the model on a straight cylindrical intake and then to investigate acoustic propagation in a large lips intake. Following this, the unsteady pressure field inside the intake is investigated more in details for given massflow and frequency. Eventually, the analytical model and numerical simulations are compared over the compressor map for various massflows and frequencies to get the whole picture.

## ANALYTICAL MODEL

The model is divided in two parts: the first one models reflection at the intake opening, and the second one models propagation inside the duct. In the following, the walls are perfectly rigid, the fluid is compressible, inviscid and perfect and the flow is subsonic, isentropic and irrotational. As on figure 1, the axial position is noted  $x$  and the radius is noted  $r$ .  $r_0$  is the reference radius, equal to the shroud radius at the fan plane.

### Reflection at the intake opening

Reflection is computed using the model developed in Rienstra (1984). The flow is assumed to be axial and uniform in a semi-infinite cylindrical duct. The model takes into account the reflection of a mode on itself and also its reflection on other modes. The result is a complex reflection coefficient  $\mathcal{R}$ , expressed as a function of the following parameters:

$$\mathcal{R} = g(M_x, kr_0, m, \mu) \quad (1)$$

Input parameters are the axial Mach number  $M_x$ , the Helmholtz number defined as the product of wave number  $k$  and shroud radius  $r_0$ , and the modal pattern  $(m, \mu)$ .  $k = 2\pi f/a$  where  $f$  is the frequency and  $a$  is the sound speed. A duct mode is defined by the couple of its azimuthal order  $m$  and its radial order  $\mu$ . Because only the first radial order (i.e.  $\mu = 0$ ) is cut-on in the following, only the azimuthal order will be mentioned from now. The acoustic azimuthal order is chosen to match with the number of nodal diameters of the mechanical mode excited by flutter.

In the following, we will consider the mean axial Mach number in the intake duct as an input for the reflection model. The axial Mach number is fixed by the geometry, the massflow  $\dot{m}$  and the farfield total pressure and total temperature.

### In-duct propagation

Based on Rienstra (1999), the acoustic pressure field inside the duct can be written as a sum of acoustic modes:

$$p(x, r, \theta, t) = \sum_{m=0}^{+\infty} p_m^\pm(x, r) e^{i(\omega t - m\theta)} \quad (2)$$

where:

$$p_m^\pm(x, r) = A_m^\pm(x) \psi_m(x, r) e^{-i \int_0^x k_x^\pm(\xi) d\xi} \quad (3)$$

$A_m^\pm(x)$  is the amplitude of the mode  $m$ .  $\psi_m(x, r)$  is the radial distribution of the mode.  $\omega = 2\pi f$  is the angular frequency. The term  $e^{i(\omega t - m\theta)}$  shows the spinning behavior of the mode, with an azimuthal velocity equal to  $\omega/m$ . The term  $e^{-i \int_0^x k_x^\pm(\xi) d\xi}$  determines the axial propagation of the mode. For a given axial position  $\xi$ , under the hypothesis that the aerodynamic field is axial and uniform in the axial section, the axial wave number is given by:

$$k_x^\pm(\xi) = \frac{-M_x(\xi)k(\xi) \pm \sqrt{k(\xi)^2 - (1 - M_x(\xi)^2)K_m(\xi)^2}}{1 - M_x(\xi)^2} \quad (4)$$

where  $k$  is the wave number and  $K_m$  is the radial wave number. The latter can be obtained considering boundary conditions at hub and shroud (see Rienstra (1999)).

Considering equation (4), the axial wave number  $k_x^\pm$  can be decomposed in two terms:

- $\frac{\pm \sqrt{k^2 - (1 - M_x^2)K_m^2}}{1 - M_x^2}$  is the propagation part. It can be real or complex. The sign in front of the square root determines the propagating direction of the wave: upstream (-) or downstream (+).
- $\frac{-M_x k}{1 - M_x^2}$  is the convected part.

If  $k_x$  is real, the mode is cut-on and propagates along the duct. If it has a non zero imaginary part, the mode is cut-off and it is exponentially attenuated as it goes through the duct. This situation occurs when the term under the square root in the propagation term is negative. That leads to the expression of the cut-on frequency as given in Zhao et al. (2017):

$$f_c = \frac{K_m a}{2\pi} \sqrt{1 - M_x^2} \quad (5)$$

To apply the model, the axial Mach number  $M_x(x)$  is needed all along the intake axis. It is calculated from massflow and section, using isentropic formulae. Besides, because section and flow are not uniform in the present study, emitted wave may be alternatively cut-on and cut-off through the duct. That is why there is not a unique cut-on frequency of the duct but a range of transitional frequencies from cut-off to cut-on. This phenomenon is not taken into account in the present model, and could be observed only in numerical simulations.

## NUMERICAL ACOUSTIC SOLVER

The solver Actran, edited by Free Field Technologies (2016), is used to make acoustic simulations in the intake. It is an acoustic Euler finite element solver. Computational domain includes the intake until the fan leading edge position, and also the upstream exterior domain to simulate properly reflection and radiation at the intake opening. The mean flow is calculated with Actran Euler solver, imposing a zero velocity potential on the freestream boundary and a given axial Mach number on fan plane. For acoustic computations, the solver considers a linearized flow. MUMPS algorithm is used to solve the finite elements linear system. Infinite elements coupled with a non reflecting condition are used on freestream boundary. A non reflecting condition is also used on fan plane, and annular duct modes (same form as in equation (2)) are imposed on the same boundary to simulate the fan as an acoustic source. Computational domain is 2D axisymmetric, and only mode  $m = 2$  is simulated. 3D simulations were also done, allowing a possible recombination on other modes, and showed a very good agreement with 2D computations without recombination. Extractions for different axial positions are done following the method in Ovenden and Rienstra (2004) thanks to the iTM tool in Actran.

## COMPARISON OF THE ANALYTICAL MODEL WITH NUMERICAL RESULTS

We chose to show results for mode  $m = 2$ . Indeed, it is representative of flutter events detected on modern fans, that mostly involve first bending mode with low nodal diameter (see Sanders et al. (2003), Aotsuka and Murooka (2014), Vahdati and Cumpsty (2016)). Hence, the acoustic mode at the fan plane is given by the frequency and the azimuthal order  $m = 2$  of the mechanical mode. In the following, we focus on two values in particular:

1. The pressure amplitude ratio at the fan plane  $\tau$  defined as the product of attenuation inside the duct between the fan plane ( $x = 0$ ) and the duct opening ( $x = x_{\text{opening}}$ ) and the reflection rate at the duct opening:

$$\tau = \frac{|p_2^+(x=0)|}{|p_2^-(x=0)|} = \frac{|p_2^-(x=x_{\text{opening}})|}{|p_2^-(x=0)|} \times |\mathcal{R}| \times \frac{|p_2^+(x=0)|}{|p_2^+(x=x_{\text{opening}})|} \quad (6)$$

2. The phase lag at the fan plane  $\Delta\phi$  between both waves  $p_2^+(x=0)$  and  $p_2^-(x=0)$ .

In the following, the reference massflow  $\dot{m}_0$  is arbitrarily chosen.

### Validation of the analytical model

To validate the model combining those of Rienstra (1984) and Rienstra (1999), a cylindrical intake with infinitely thin lips is considered. Thus, the configuration suits the hypotheses for the reflection model. Because this configuration is not possible in Actran, a sharp edge is used instead to reproduce the same behavior, like in Druon (2006). The base mean flow is taken uniform.

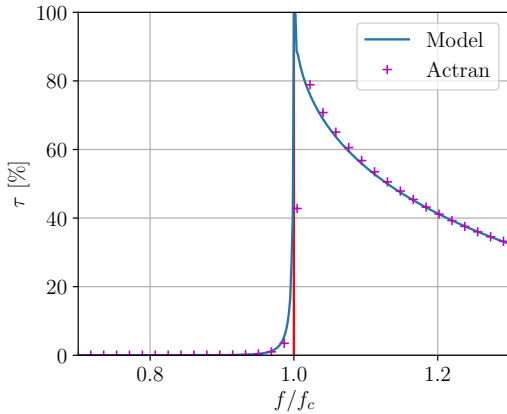


Figure 2: **Pressure amplitude ratio as a function of normalized frequency for  $\dot{m} = \dot{m}_0$  (cylindrical intake)**

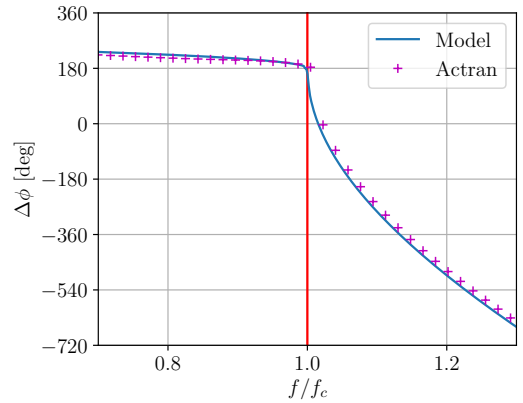


Figure 3: **Phase lag as a function of normalized frequency for  $\dot{m} = \dot{m}_0$  (cylindrical intake)**

Figures 2 and 3 show respectively the pressure amplitude ratio and the phase lag at fan plane as a function of frequency normalized by the analytical cut-on frequency  $f_c$  (see equation (5)). Because acoustic driven flutter is expected to happen near and above cut-on frequency (see Vahdati et al. (2015)), frequency range is limited to  $1.3f_c$ .

For low frequencies, the mode  $m = 2$  is cut-off in the intake. The pressure amplitude ratio is very close to zero. When frequency increases to be close to the cut-on frequency,

the mode becomes suddenly cut-on and  $\tau$  soars to 100%. Phase lag derivative becomes also important, because the dominant term is due to propagation. As frequency increases above cut-on frequency, the pressure amplitude ratio decreases and the phase lag keeps the same slope.

There is a very good agreement between the model and Actran results. The cut-on frequency is well predicted, and the pressure amplitude ratio and the phase lag are also compliant. The analytical model is then performant when it is applied on a test case matching all the hypotheses.

### Application on an intake with large lips

The model is now applied on an intake with large lips shown on figure 4. This intake ge-

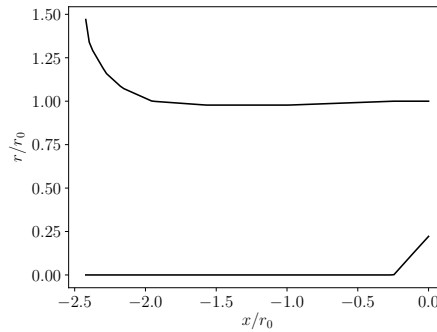


Figure 4: **Intake geometry with large lips**

ometry deviates from model hypotheses in particular because of lips shape and quickly varying section near the intake opening. Lidoine et al. (2001) showed that this shape makes the mode be more radiated in the axial direction. Hence, it is likely that it also impacts the reflection mechanism. Moreover, the region around  $x/r_0 = -0.25$  near the spinner could be a zone where radial gradients are not negligible anymore.

#### Effect of frequency

First, the evolution of pressure amplitude ratio and phase lag with frequency is investigated. Results are shown on figures 5, 6 and 7. Because of the variable section of the intake, cut-on frequency varies between the fan plane and the intake opening. On the figures,  $f_c$  is the average of cut-on frequencies at each section along the duct.

Comparing the model to Actran results leads to the following conclusions:

- The averaged cut-on frequency is well predicted by the model.
- The model underestimates the pressure amplitude ratio below cut-on frequency and overestimates it above. For  $f < f_c$ , the model considers that the outgoing wave is completely cut-off, although it could propagate with a moderated attenuation. For  $f > f_c$ , reflection at the intake opening is not well captured, because the shape of the duct does not fit the model hypotheses.
- Phase lag is not well predicted around cut-on frequency, nor above  $1.2f_c$ . However model is quite satisfactory between  $1.05f_c$  and  $1.2f_c$ , with a maximum error around 45 degrees. This frequency range is the most crucial because the mode is cut-on with a quite high

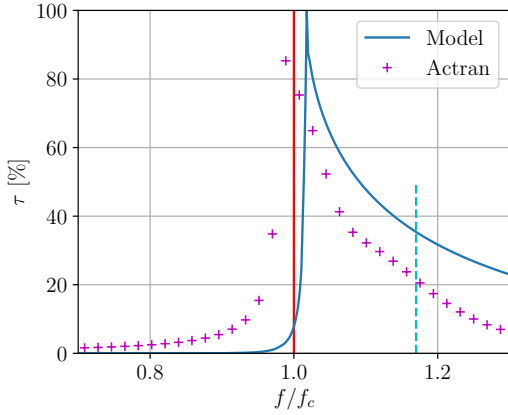


Figure 5: **Pressure amplitude ratio as a function of normalized frequency for  $\dot{m} = \dot{m}_0$  (large lips intake). The cyan vertical dashed line is located at  $f = 1.17f_c$ .**

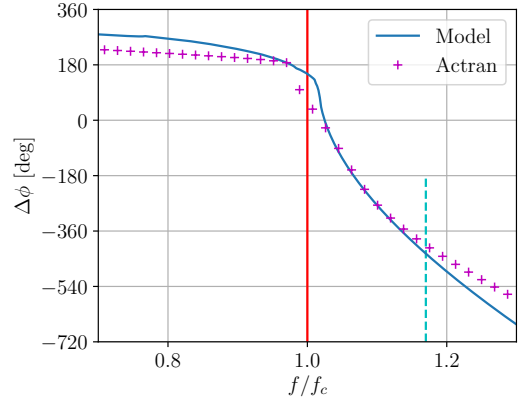


Figure 6: **Phase lag as a function of normalized frequency for  $\dot{m} = \dot{m}_0$  (large lips intake). The cyan vertical dashed line is located at  $f = 1.17f_c$ .**

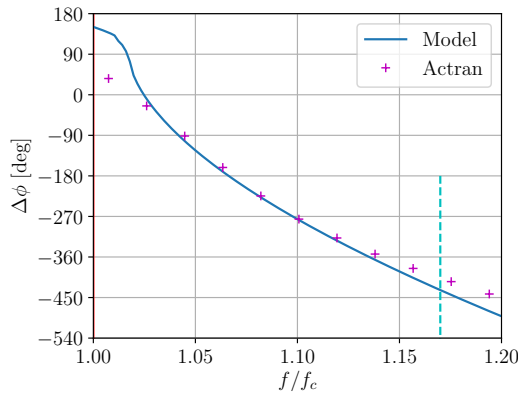


Figure 7: **Zoom of figure 6: Phase lag as a function of normalized frequency for  $\dot{m} = \dot{m}_0$  (large lips intake). The cyan vertical dashed line is located at  $f = 1.17f_c$ .**

pressure amplitude ratio. Hence, it is the range where the intake is expected to have the greatest impact on fan flutter.

#### Unsteady pressure field inside the large lips intake

Figures 8 to 11 show the unsteady pressure field inside the intake, obtained with the model and Actran at  $\dot{m} = \dot{m}_0$  and  $f = 1.17f_c$ . This operating point corresponds to an extraction on the cyan vertical dashed line on figures 5 to 7. The abscissa variable is the same as on figure 4. The presented unsteady pressure is the superposition of the outgoing wave  $p^-$  and the reflected incoming wave  $p^+$ . Both fields are similar, except near the intake opening where shroud curvature is important. Several observations can be made:

- The mode  $m = 2$  propagates mostly near the shroud. It is a consequence of the radial distribution  $\psi_m(x, r)$  in equation (3).

- Between  $x/r_0 = -2$  and  $x/r_0 = -0.5$ , the pressure phase in Actran simulation depends only on  $x$ , which is one of the model hypotheses. The  $\Delta\phi = \pm 180^\circ$  line is located at  $x/r_0 = -0.9$  for Actran and model results. However, constant phase lines in the Actran result field are curved near the intake opening and near the spinner.
- The axial alternated pattern in amplitude is the result of the interferences between the outgoing and incoming waves.

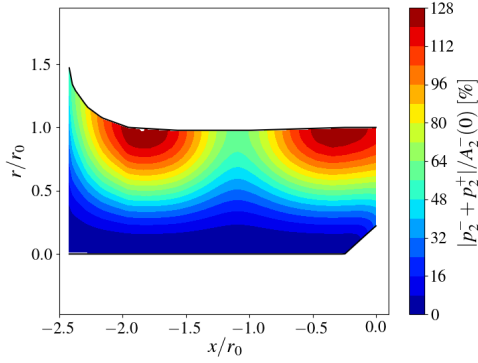


Figure 8: **Unsteady pressure amplitude for the analytical model.**  $\dot{m} = \dot{m}_0$  and  $f = 1.17f_c$  (large lips intake)

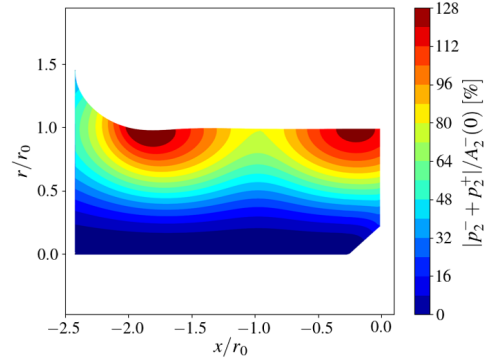


Figure 9: **Unsteady pressure amplitude for Actran simulations.**  $\dot{m} = \dot{m}_0$  and  $f = 1.17f_c$  (large lips intake)

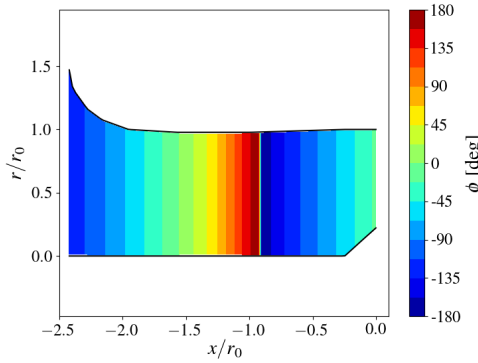


Figure 10: **Unsteady pressure phase lag for the analytical model.**  $\dot{m} = \dot{m}_0$  and  $f = 1.17f_c$  (large lips intake)

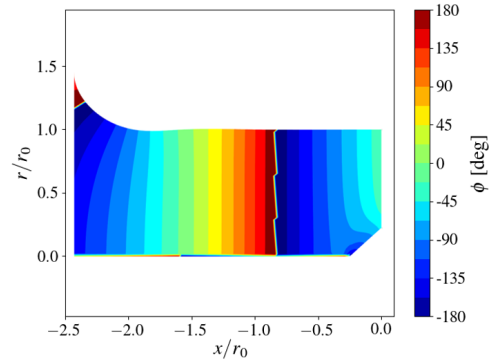


Figure 11: **Unsteady pressure phase for Actran simulations.**  $\dot{m} = \dot{m}_0$  and  $f = 1.17f_c$  (large lips intake)

To go further in the analysis, unsteady pressure is decomposed into the outgoing and incoming waves. These two parts are directly known in the analytical model. For Actran simulations, they are obtained with the iTM tool. Figures 12 and 13 show the evolution of amplitude and phase of unsteady pressure inside the intake, between the fan leading edge and the duct opening. Both the outgoing and incoming waves are featured. The amplitude is the term  $A_2^\pm(x)$  in equation (3) normalized by the outgoing amplitude at the fan plane  $A_2^-(0)$ . The phase  $\phi^\pm$  is the

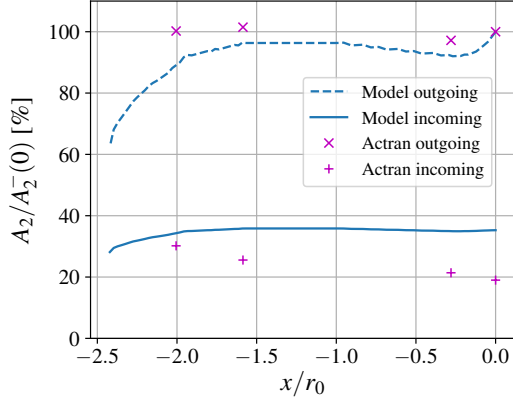


Figure 12: **Unsteady pressure amplitude as a function of axial position between fan plane ( $x/r_0 = 0$ ) and the inlet ( $x/r_0 \approx -2.5$ ).  $\dot{m} = \dot{m}_0$  and  $f = 1.17f_c$  (large lips intake)**

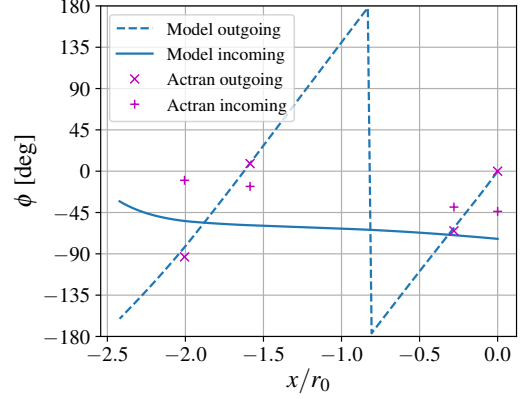


Figure 13: **Unsteady pressure phase as a function of axial position between fan plane ( $x/r_0 = 0$ ) and the inlet ( $x/r_0 \approx -2.5$ ).  $\dot{m} = \dot{m}_0$  and  $f = 1.17f_c$  (large lips intake)**

argument of  $p_2^\pm$  in the same equation. We can notice that the value  $A_2^+(0)/A_2^-(0)$  on figure 12 is equal to the pressure amplitude ratio that can be read on figure 5.

Amplitude and phase of the outgoing wave are well predicted by the model. However, there is a gap between model and Actran results for the reflected wave. On figure 12, unsteady pressure amplitude is almost constant for both the outgoing and incoming waves, except near the intake opening where the model predicts a decrease. For the incoming wave, Actran gives a small decrease of the amplitude all along the duct, whereas the model predicts a nearly constant amplitude and thus overestimates the pressure amplitude ratio at the fan plane ( $x/r_0 = 0$ ). This difference could be explained by a defect in reflection modelling or in propagation modelling for the incoming wave. A possible source of error is the axial Mach number taken as an input by the model near the intake opening (see equation (4)). Indeed, it considers an averaged Mach number on the axial section, computed with isentropic formulae. Because section increases quickly near the intake opening, unsteady pressure amplitude decreases in the upstream direction and increases in the downstream direction. However, the mode  $m = 2$  propagates mostly near the shroud (see figures 8 and 9), and lips curvature induces an acceleration of the flow at the intake opening. It can be seen on the mean Mach number field used in Actran simulations, presented on figure 14. As a result, a possible explanation of the gap between Actran results and the model is that, near the intake opening, this mode sees a decrease of Mach number in the model but an increase in Actran simulations.

A possible solution could be to use the model with an axial Mach number extracted around 90% of shroud radius in a throughflow computation. It will impact equations (1) and (4).

The same analysis can be applied for phase results on figure 13. Phase slope is correctly predicted for outgoing and incoming waves, but local defect of the model around the intake opening leads to a constant phase shift for the incoming wave.

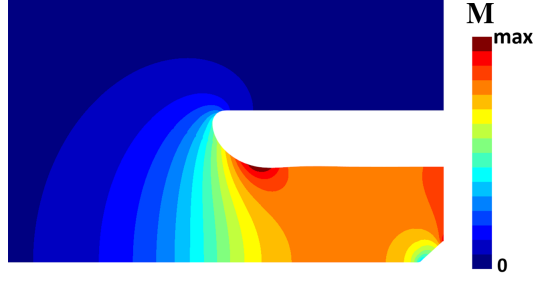


Figure 14: **Mean Mach number field for Actran simulation for  $\dot{m} = \dot{m}_0$**

*Results over the compressor map for the large lips intake*

Figures 15 to 18 present the pressure amplitude ratio and the phase lag on the compressor map as a function of massflow and frequency of the first bending mode of the fan blade, for analytical and Actran results. Frequency is normalized by the cut-on frequency, depending on the massflow. Results are shown over accessible operating points, classically associated with a given massflow and a given rotating speed. Actran results are interpolated from the points identified by black crosses. Results obtained with the analytical model are computed on a refined grid (6 times on the x-axis and 4 times on the y-axis). Cut-on frequency is featured with a solid red line. One may notice than results presented on figures 5 and 6 are extractions along the vertical dashed lines featured on figures 15 to 18.

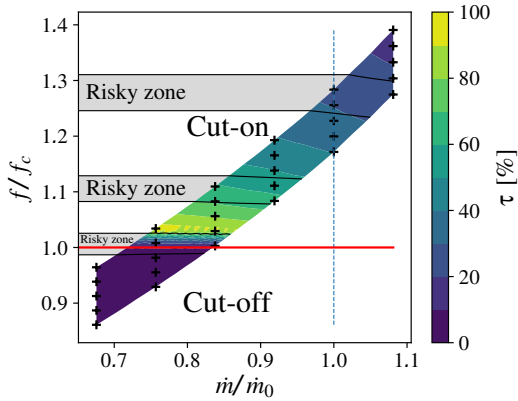


Figure 15: **Pressure amplitude ratio over the fan map for the analytical model**

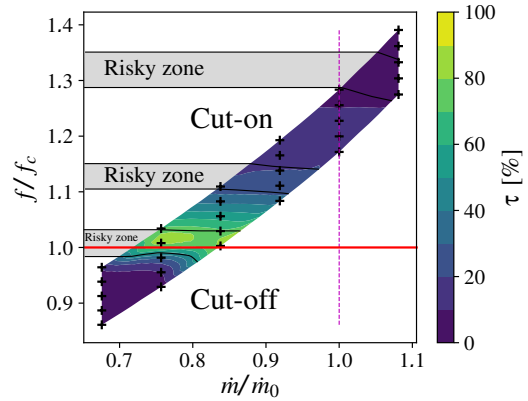


Figure 16: **Pressure amplitude ratio over the fan map for Actran simulations**

Previous observations can be generalized over the compressor map. The model overestimates the pressure amplitude ratio, but transition from cut-off to cut-on as frequency increases matches with Actran results. Besides, although phase lag is less correctly estimated for higher frequencies than near cut-on frequency, it is possible to locate quite accurately risky zones over the fan map where phase lag is around  $90^\circ$  (zones featured as grey areas on figures 15 to 18). According to Vahdati et al. (2015), this phase lag corresponds to conditions where the intake is the more destabilizing for fan flutter. The error for higher frequencies is not so important because the pressure amplitude ratio is quite low. It is good to notice that the pressure amplitude ratio could have an amplifying effect on flutter, but phase is decisive on the presence of flutter

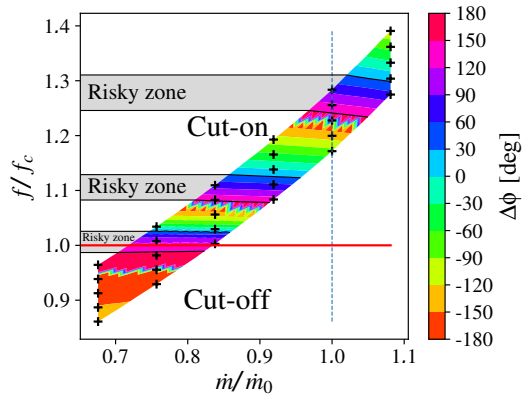


Figure 17: **Phase lag over the fan map for the analytical model**

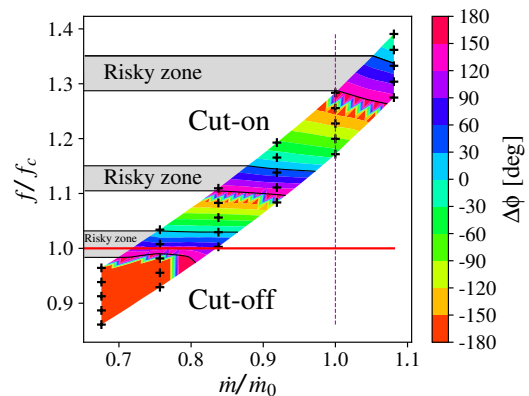


Figure 18: **Phase lag over the fan map for Actran simulations**

or not.

## CONCLUSIONS

An analytical model has been used to predict the pressure amplitude ratio and the phase lag of an acoustic wave emitted by fan flutter and reflected by the intake opening. It has been compared with results of simulations with the acoustic solver Actran. The model has been validated for a cylindrical intake with a uniform mean flow. Thereafter, it has been tested for an intake with large lips. For this case, it has been shown that:

- The analytical model gives a fast and good approximation of cut-on frequency.
- Above cut-on frequency, the model overestimates the pressure amplitude ratio. It is probably due to the curved shape of the intake lips. Indeed, acoustics waves do not have the same behavior around a wedge and a thick rounded edge.
- Model predicts the phase lag with a low precision. Nonetheless, it is enough to locate risky zones over the compressor map.

Imposing an axial Mach number extracted near the shroud from a throughflow computation could improve modelling, mostly around the intake opening. Model could also be improved by taking into account the complex behavior of waves around cut-on frequency, switching between cut-on and cut-off regions all along the intake.

Another aspect is that neither the analytical model nor Actran simulations take into account the interaction of duct modes with the near field and aerodynamic structures around the blade. To do that, future works should use Navier-Stokes 3D computations to focus on the links between acoustic and flutter bite. The feed-back of the acoustic reflected wave on pressure field around the leading edge should be particularly explored.

## ACKNOWLEDGEMENTS

The authors thank Safran Aircraft Engines for sponsoring this work and allowing its publication.

## REFERENCES

- Aotsuka, M. and Murooka, T. (2014). Numerical Analysis of Fan Transonic Stall Flutter. In *ASME Turbo Expo 2014*, Dusseldorf, Germany.
- Druon, Y. (2006). *Etude de la propagation guidée et du rayonnement acoustiques par les conduits d'éjection de turboréacteur*. PhD thesis, Ecole Centrale de Lyon.
- Free Field Technologies, . (2016). *ACTRAN 17 User's Guide - Volume 1 : Installation, Operations, Theory and Utilities*.
- Lidoine, S., Batard, H., Troyes, S., Delnevo, A., and Roger, M. (2001). Acoustic radiation modelling of aeroengine intake comparison between analytical and numerical methods. *7th AIAA/CEAS Aeroacoustics Conference and Exhibit*.
- Ovenden, N. C. and Rienstra, S. W. (2004). Mode-Matching Strategies in Slowly Varying Engine Ducts. *AIAA Journal*, 42(9):1832–1840.
- Rienstra, S. (1999). Sound transmission in slowly varying circular and annular lined ducts with flow. *Journal of Fluid Mechanics*, 380:279–296.
- Rienstra, S. W. (1984). Acoustic radiation from a semi-infinite annular duct in a uniform subsonic mean flow. *Journal of Sound and Vibration*, 94(2):267–288.
- Sanders, A. J., Hassan, K. K., and Rabe, D. C. (2003). Experimental and Numerical Study of Stall Flutter in a Transonic Low-Aspect Ratio Fan Blisk. In *ASME Turbo Expo 2003*, Atlanta, Georgia, USA.
- Vahdati, M. and Cumpsty, N. (2016). Aeroelastic Instability in Transonic Fans. *Journal of Engineering for Gas Turbines and Power*, 138(2):022604.
- Vahdati, M., Simpson, G., and Imregun, M. (2011). Mechanisms for Wide-Chord Fan Blade Flutter. *Journal of Turbomachinery*, 133(4).
- Vahdati, M., Smith, N., and Zhao, F. (2015). Influence of intake on fan blade flutter. *Journal of Turbomachinery*, 137(8).
- Vallon, A., Herran, M., Ficat-Andrieu, V., and Detandt, Y. (2018). Numerical investigations of flutter phenomenon in compressor stages of helicopter engines. In *2018 AIAA/CEAS Aeroacoustics Conference*. American Institute of Aeronautics and Astronautics.
- Whitehead, D. S. (1973). The Effect of Compressibility on Unstalled Torsional Flutter. Technical Report 3754, Aeronautical Research Council reports and memoranda.
- Zhao, F., Smith, N., and Vahdati, M. (2017). A Simple Model for Identifying the Flutter Bite of Fan Blades. *Journal of Turbomachinery*, 139(7):071003–071003–10.